

Mid-Infrared Slow-Light Photonic Breath Sensor for Early Lung Cancer Screening

May Hlaing^{1,2*}, Jia Zheng Bao¹, Kang-Chieh Fan¹, Jason Midkiff^{1,2}, Sourabh Jain¹, Donglei-Emma Fan¹ and Ray T. Chen^{1,2}

¹Department of Electrical and Computer Engineering, University of Texas at Austin, TX 78758, USA

²Omega Optics, Inc., 8500 Shoal Creek Blvd., Bldg. 4, Suite 200, Austin, Texas 78757, USA

*Author e-mail address: may.hlaing@omegaoptics.com

Abstract: A mid-infrared silicon vertical photonic crystal waveguide with engineered slow-light dispersion ($n_g \approx 1064$) enhances the acetaldehyde absorption near 5.88 μm , enabling compact exhaled-breath sensor designs for early lung cancer detection. © 2026 The Author(s)

1. Introduction

Early detection of lung cancer is critically important for improving patient outcomes, creating a need for sensing technologies capable of detecting trace-level biomarkers in human exhaled breath. Several volatile organic compounds (VOCs) linked to metabolic pathways, including acetaldehyde ($\text{C}_2\text{H}_4\text{O}$), acetone ($\text{C}_3\text{H}_6\text{O}$), and formaldehyde (HCHO), have been investigated as potential indicators of lung disease [1-3]. These species exhibit mid-infrared (mid-IR) absorption features near 5.7–5.8 μm corresponding to carbonyl ($\text{C}=\text{O}$) stretching modes. Mid-IR spectroscopy is well suited for detecting such biomarkers because it probes their fundamental vibrational-rotational transitions, which are significantly stronger than near-infrared overtone bands. However, conventional mid-IR spectroscopic tools such as cavity ring-down spectroscopy (CRDS), tunable diode laser absorption spectroscopy (TDLAS), and photoacoustic spectroscopy (PAS) rely on long free-space optical paths and precise alignment components, limiting their suitability for compact, point-of-care uses. Integrated photonic platforms provide a path toward miniaturized absorption spectroscopy. Photonic crystal waveguides can be engineered to operate in slow-light regime near the photonic band edge, where the group velocity $v_g = \frac{c}{n_g}$ is significantly reduced [4-5]. Hence, the large group index n_g increases the light-matter interaction with the analyte. On-chip absorption modifies the Beer–Lambert relation as, $I = I_0 \exp(-\Gamma \alpha n_g L)$, $\Gamma = f \frac{c}{v_g}$, where I and I_0 are the transmitted and incident intensities, α is the analyte absorption coefficient, L is the physical propagation length, Γ is a dispersion-dependent enhancement factor [6-7], f is the filling factor representing the fraction of modal energy overlapping the analyte. Slow-light with a large n_g therefore enables strong absorption even for short device lengths (on the order of hundred micrometers).

In this work, we numerically investigated a Si-based vertical photonic crystal waveguide (VPCW) designed to align its band-edge slow-light mode with the $\text{C}_2\text{H}_4\text{O}$ absorption near 5.88 μm . Using plane-wave expansion (PWE) and 3D finite-difference time-domain (FDTD) simulations, we evaluate the dispersion, group index, modal field properties, and absorption enhancement. The optimized design demonstrates strong slow-light behavior with a calculated group index $n_g \approx 1064$. Normal incidence mid-IR measurements confirm the appearance of a sharp band-edge resonance whose spectral position agrees with simulation, suggesting the presence of slow-light behavior in the fabricated VPCW. These combined numerical and experimental results demonstrate the potential of VPCWs for compact, chip-scale mid-IR sensing of breath biomarkers relevant to lung-cancer screening and early diagnostics.

2. Device Design, Numerical Simulation, Fabrication and Results

The VPCW device (Fig. 1a) is based on a two-dimensional (2D) hexagonal photonic crystal formed by etching a periodic lattice of air holes into a silicon slab and introducing a single hollow-core defect to support guided modes. The optimized lattice constant $a = 2.463 \mu\text{m}$ and radius ratio $\frac{r}{a} \approx 0.43$ produce a complete photonic bandgap spanning 5.88–6.05 μm . The defect radius $R_{\text{defect}} \approx 3.11a$ is tuned to align the band-edge resonance with the 5.88 μm acetaldehyde absorption feature. The active sensing region has a compact footprint defined by the ~140- μm vertical etched depth and ~35- μm lateral width. Band structures were computed using the plane-wave expansion (PWE) method in RSoft BandSOLVE, and modal confinement and dispersion were evaluated using Lumerical

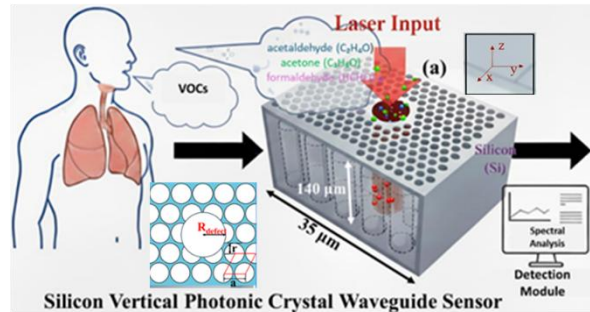


Fig.1 Schematic of the silicon VPCW breath sensor. Exhaled VOCs interact with the hollow-core defect, where slow-light enhances mid-IR absorption for compact spectral detection.

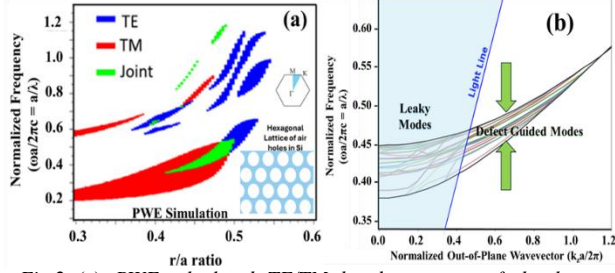


Fig.2 (a) PWE-calculated TE/TM band structure of the hexagonal photonic crystal showing a complete bandgap near the target wavelength. (b) Out-of-plane dispersion of the defect-engineered VPCW, highlighting well-confined defect-guided modes below the light line.

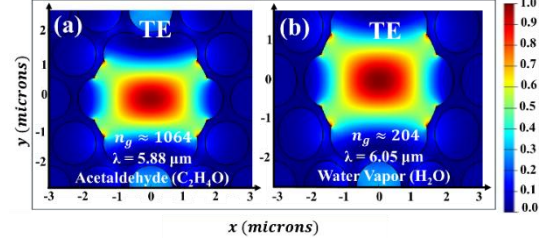


Fig. 3. Transverse electric (TE) field profiles of air-core defect modes in the vertical photonic crystal waveguide. (a) Slow-light defect mode tuned to the C₂H₄O absorption band with $n_g \approx 1064$. (b) Slow-light defect mode tuned to the H₂O absorption band ($n_g \approx 204$).

3D FDTD simulations. **Fig. 2a** shows both transverse electric (TE) and transverse magnetic (TM) bandgaps and the defect-mode dispersion. The PWE results indicate a photonic bandgap of $\lambda_{\text{PBG}} \approx 5.88\text{--}6.05 \mu\text{m}$, within which defect-guided modes appear below the light line. Out-of-plane dispersion characteristics (**Fig. 2b**) show that the defect breaks the in-plane periodicity and introduces guided modes within the bandgap. Near $k_z = 0$, TE and TM bands remain distinct. For $k_z \neq 0$, the modes hybridize and form an ultra-flat dispersion near the band edge, indicating large group indices and strong slow-light behavior. Below the light line, these defect-guided modes remain well confined with minimal radiation leakage. The high index contrast of the silicon platform enables broader and more stable bandgaps than low-index silica-based photonic crystal fiber structures. The simulated field distribution (**Fig. 3**) shows strong mode confinement with large group indices within the defect hollow core, yielding a high filling factor suitable for gas sensing. VPCW arrays were fabricated on double-side-polished silicon wafers using electron-beam lithography, SiO₂ hard-mask patterning, and Bosch deep reactive-ion etching, yielding 1.3–1.5 μm air-hole diameters ($r/a \approx 0.43$) and ± 20 nm defect-radius accuracy.

Fabricated VPCW devices were characterized using a Bruker Vertex v80 FTIR microscope over the 4–10 μm range. Measurements were performed under N₂ purge with baseline subtraction to reduce atmospheric absorption. Reflectance spectra collected from the defect region show clear resonances near 5.88 μm and 6.05 μm, consistent with simulated band-edge modes (**Fig. 4b**). The resonances display sharp band-edge resonance features characteristic of slow-light behavior, with linewidth variations arising from fabrication tolerances and finite-array effects. The resonance wavelengths shift predictably with defect radius, confirming the design approach for aligning photonic resonances with target absorption bands. The Fano resonance near 6.05 μm is designed because water (H₂O) often overlaps with VOC signatures in the 6 μm range. This sharp Fano-sensitive feature enables tracking and compensation of water-induced spectral shifts [8–9].

Conclusion: A silicon vertical photonic crystal waveguide was designed and numerically evaluated for slow-light-enhanced mid-IR sensing of acetaldehyde near 5.88 μm. The optimized structure supports a high-index band-edge mode ($n_g \approx 1064$) with strong field confinement in an air-core defect, providing substantial absorption enhancement within a compact device footprint. These results demonstrate the suitability of silicon VPCWs for integrated breath-analysis platforms targeting early lung-cancer detection. The authors acknowledge and thank NASA for supporting this work under contract number **80NSSC22PC125**.

References:

[1] M. Phillips et al., *J. Breath Res.* 4, 026003 (2010).
 [2] D. Smith and P. Španěl, *TrAC* 30, 345–352 (2011).
 [3] G. N. Walker et al., *Appl. Spectrosc.* 72, 129–144 (2018).
 [4] D. Mori et al., *Opt. Express*, 15, 5264–5270 (2007).
 [5] W.-C. Lai et al., *Appl. Phys. Lett.*, 102, 041111 (2013).
 [6] C.-Y. Lin et al., *Opt. Lett.*, 37, 232–234 (2012).

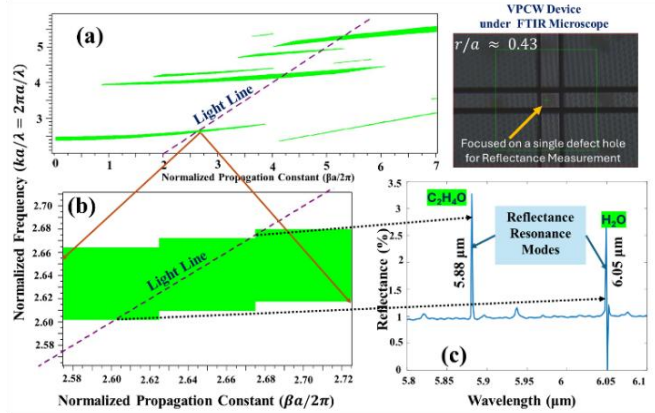


Fig.4 (a) Projected out-of-plane band diagram of the silicon VPCW showing guided and leaky modes relative to the light line. (b) Magnified view highlighting the defect-guided band-edge region (5.88–6.05 μm). (c) Measured reflectance spectra from a single defect hole, showing resonances at $\sim 5.88 \mu\text{m}$ and $\sim 6.05 \mu\text{m}$. An SEM image of the fabricated device is shown at top right.

[7] W. Zhou et al., *Prog. Quantum Electron.*, 38, 1–74 (2014).
 [8] S. M. Sherif et al., “Silicon double-Fano photonic integrated gas sensor,” *J. Lightwave Technol.*, 42, 5194–5202 (2024).
 [9] S. E. Zaki et al., “Fano-resonant defect 1D photonic crystal for gas sensing,” *Sci. Rep.*, 10, 17979 (2020).